INTERNATIONAL JOURNAL OF HYPERTHERMIA
2019, VOL. 36, NO. 1, 676–685
https://doi.org/10.1080/02656736.2019.1627585

Taylor & Francis
Taylor & Francis Group

Development of a catheter-based technique for endoluminal radiofrequency sealing of pancreatic duct

Elżbieta Ewertowska[a], Anna Andaluz[b], Xavier Moll[b], Adrià Aguilar[b], Felix Garcia[b], Dolors Fondevila[b], Rita Quesada[c], Macarena Trujillo[d], Fernando Burdío[e] and Enrique Berjano[a]

[a]BioMIT, Department of Electronic Engineering, Universitat Politècnica de València, Valencia, Spain; [b]Departament de Medicina i Cirurgia Animals, Facultat de Veterinària, Universitat Autònoma de Barcelona, Barcelona, Spain; [c]Department of Experimental and Health Sciences, Universitat Pompeu Fabra, Barcelona, Spain; [d]BioMIT, Department of Applied Mathematics, Universitat Politècnica de València, València, Spain; [e]Department of Surgery, Hospital del Mar, Barcelona, Spain

ABSTRACT

Introduction: Endoluminal sealing of the pancreatic duct by glue or sutures facilitates the management of the pancreatic stump. Our objective was to develop a catheter-based alternative for endoluminal radiofrequency (RF) sealing of the pancreatic duct.

Materials and methods: We devised a novel RF ablation technique based on impedance-guided catheter pullback. First, bench tests were performed on *ex vivo* models to tune up the technique before the *in vivo* study, after which endoluminal RF sealing of a ~10 cm non-transected pancreatic duct was conducted on porcine models using a 3 Fr catheter. After 30 days, sealing effectiveness was assessed by a permeability test and a histological analysis.

Results: The RF technique was feasible in all cases and delivered ~5 W of power on an initial impedance of 308 ± 60 Ω. Electrical impedance evolution was similar in all cases and provided guidance for modulating the pullback speed to avoid tissue sticking and achieve a continuous lesion. During the follow-up the animals rate of weight gain was significantly reduced ($p < 0.05$). Apart from signs of exocrine atrophy, no other postoperative complications were found. At necropsy, the permeability test failed and the catheter could not be reintroduced endoluminally, confirming that sealing had been successful. The histological analysis revealed a homogeneous exocrine atrophy along the ablated segment in all the animals.

Conclusions: Catheter-based RF ablation could be used effectively and safely for endoluminal sealing of the pancreatic duct. The findings suggest that a fully continuous lesion may not be required to obtain complete exocrine atrophy.

ARTICLE HISTORY
Received 17 November 2018
Revised 20 May 2019
Accepted 31 May 2019

KEYWORDS
Ablation; endoluminal; pancreatic duct; radiofrequency; sealing

1. Introduction

Sealing of the pancreatic duct is used to manage two main pancreatic malignancies: pancreatitis and pancreatic ductal adenocarcinoma [1]. Sealing is usually achieved either by ligation of the affected pancreatic duct to eliminate pancreatic secretions or tumor resection followed by anastomosis of the remaining pancreatic stump [2,3]. However, the common problem of leakage of the pancreatic contents into the abdomen, also known as pancreatic fistula, can affect patient morbidity and mortality during the postoperative period. Many studies have explored feasible techniques for sealing the pancreatic stump in order to replace anastomosis and minimize the risk of leakage [4]. Sutures, staplers, clips or endoluminal glue injections are some of the most frequently used tools currently used in clinical practice. However, none of these techniques has been proven to effectively reduce the high risk of failure in these cases.

Radiofrequency ablation (RFA) is one of the recently explored sealing techniques. In this case the action mechanism does not rely on introducing a sealing agent, but on inducing epithelial necrosis to trigger fibrosis (cicatrization) and collagen shrinkage and cause ductal atrophy. Our research group had already examined the effect of pancreatic stump closure by RF-assisted transection in terms of fistula formation on rat and pig models [5–7]. The results showed that RFA not only induced exocrine atrophy for ductal occlusion but also reduced the occurrence of fistula. These findings encouraged us to go beyond the transection plane and consider extending RFA endoluminally along a segment of the pancreatic duct itself.

The concept of endoluminal thermal ablation is not really new since it has already been used in clinical applications for vascular occlusion such as e.g. hepatic tumor arteries, varicose veins [8,9] and biliary tumors [10]. However, to our knowledge, there is no evidence that this technique has

CONTACT Enrique Berjano eberjano@eln.upv.es Department of Electronic Engineering, Universitat Politècnica de València, (Building 7F), Camino de Vera, 46022 Valencia, Spain

been previously employed for pancreatic remnant sealing, as proposed here. As in the case of glue, the main purpose of thermal coagulation of the duct walls is to prevent leakage by sealing the secretory ducts along its walls and inducing ductal atrophy and also ensure the loss of ductal permeability. In order to efficiently perform endoluminal ablation of the pancreas, a thermal coagulation zone should meet the following characteristics: (1) it should be long enough to suit the remnant pancreas after a resection; (2) be as contiguous as possible, i.e. with the minimum number and length of gaps; (3) there should be sufficient margin across the duct wall, i.e. ablate the entire epithelium and ensure loss of permeability, which requires a depth of 1–2 mm; and (4) it must be safe, i.e. no steam pops or tissue disruption, which means keeping tissue temperature below 80–90 °C and avoiding tissue sticking to the electrode.

Additional technical requirements for a device aimed at endoluminal surgery of the pancreatic duct should also include: (1) a suitable diameter to fit the duct along the entire route; (2) flexible enough to pass easily through the duct, which is not usually straight; and (3) be long enough to cover the entire target segment. The electrodes used to create the thermal lesion should be on the catheter itself. In this context, our objective was thus to develop a new catheter-based technique for endoluminal RF sealing of the pancreatic duct and to assess its safety and performance on an *in vivo* porcine model.

2. Materials and methods

The first phase, based on an *ex vivo* model, was used to tune up the experimental setup, which consisted of an RF catheter combined with impedance-guided pullback. The aim was to determine the suitability of the catheter in terms of diameter, size, flexibility, and ablation protocol. The second phase was based on an *in vivo* porcine model and assessed the safety and feasibility of the novel technique with a 30-day follow-up. In both phases the electrodes were powered by a Radionics Cosman Coagulator CC-1 (Radionics, Burlington, MA, USA), a versatile generator previously used with endovascular RF catheters for arterial occlusion in liver cancer [8]. Impedance evolution was recorded during the ablations by a USB data acquisition module connected to the RF generator.

2.1. Tissue samples for ex vivo and in vivo models

The *in vivo* study was conducted on 8 Landrace-Large White pigs (27.3 kg mean weight), according to the protocol approved by Ethical Commission of the Universitat Autònoma de Barcelona (Authorization Number CEEAH 3487 and DMAH 9583) and the Government of Catalonia's Animal Care Committee. The *ex vivo* study was conducted on two types of sample: bovine liver acquired from a local slaughterhouse, and porcine pancreas obtained from 3 pigs, which underwent necropsy under the same authorized protocol as that used in the *in vivo* study.

2.2. Considerations on the catheter design

In general, successful endoluminal ablation should ensure: (1) catheter flexibility to operate inside the duct, (2) shallow thermal lesions circumscribed exclusively to the tissue around the pancreatic duct (sufficient to completely seal the secondary ducts draining into the main duct), and (3) the ability to estimate a suitable level of applied voltage from the initial impedance measurement. Potential catheter designs for endoluminal ablation should also take the following issues into account: number of electrodes (single or multiple), function mode (mono-, bi-, multi-polar), electrode type (dry or wet), and application procedure (point-to-point or continuous pullback).

The first tentative test was on a single long RF electrode based on a 3 Fr metallic guide whose length was tailored to the lesion length in order to create one long lesion by 'segmental' ablation. This first idea was discarded since the edge effect prevented the formation of a long uniform thermal lesion around one RF electrode. Regardless of the ablation time (10–20 s), the lesion surrounding the electrode was nonhomogeneous and much deeper at the edges, which was associated with overheating, audible steam pops (registered at 2–4 s) and tissue sticking. Also, the long metal wire was not sufficiently flexible to operate inside soft delicate tissue. Another consideration was that a single long RF electrode must be operated in monopolar mode, making it difficult to predict the thermal lesion geometry, since the exact power delivered to the target site depends on the unpredictable electrical characteristics of all the tissues involved in the electrical circuit.

The bipolar mode employs at least two closely spaced electrodes to create shallow thermal lesions confined to the inter-electrode space. The applied power depends almost exclusively on the characteristics of the tissue between the electrodes. Less power is required in bipolar mode to ablate the same lesion volume, which is appropriate in terms of safety, especially when working on small or fragile organs, such as the pancreas, which is surrounded by other delicate organs.

A final issue to be considered is the possible internal cooling of the electrodes. Although cooled electrodes have an advantage over dry electrodes and avoid tissue sticking (e.g. CelonProSurge Applicator, Olympus, Germany), they are also known to create deeper thermal lesions than the dry type. As the goal in endoluminal ablation is to create relatively shallow thermal lesions around the pancreatic duct (1–2 mm depth) and avoid damage to the pancreatic parenchyma or adjacent organs, dry electrodes seem to be the better choice.

For all the procedures we employed commercially available flexible catheters, which include a pair of metal electrodes separated by plastic insulation. The catheter would be introduced into the pancreatic duct through the papilla and would create thermal lesions around the electrodes, as illustrated in Figure 1. The lesions could be created either point-to-point (i.e. positioning the catheter at one point and then repositioning it to a contiguous point after having created a lesion) or continuously by the pullback technique.

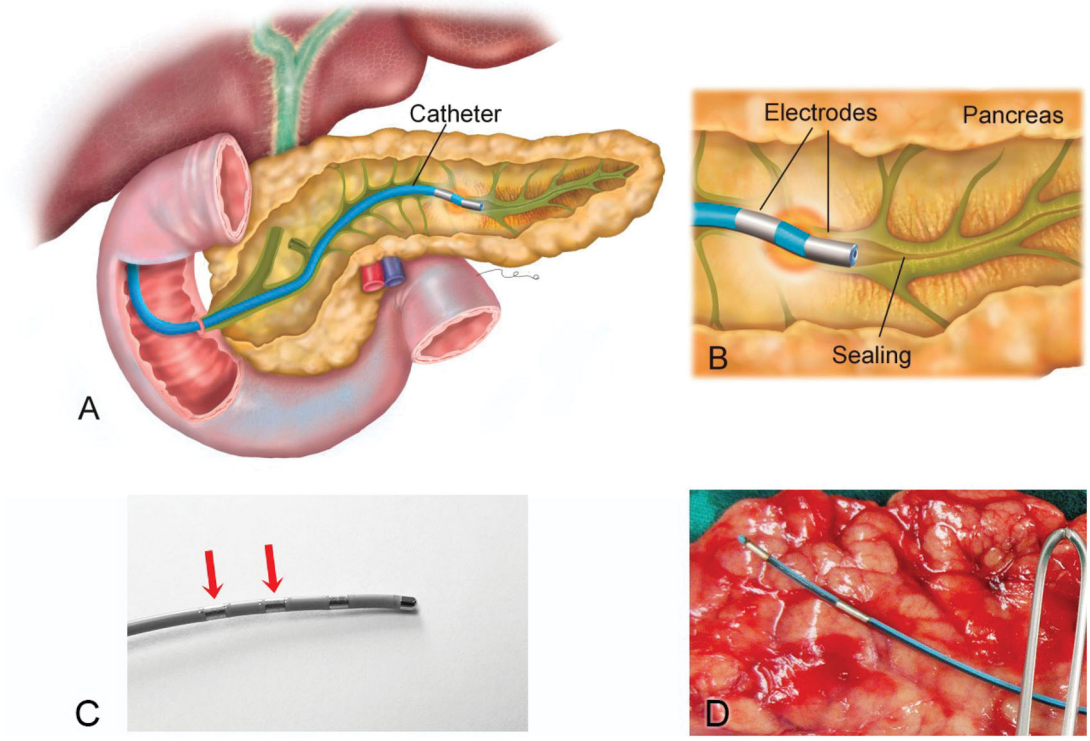

Figure 1. (A) Overview of the catheter-based technique for endoluminal radiofrequency sealing of pancreatic duct. The catheter is introduced into the pancreatic duct through the papilla. (B) Detail of catheter tip in which RF power is applied between two electrodes. The thermal lesion causes the duct to seal (the illustration is that of a human pancreas). (C) 5 Fr bipolar RF catheter used for ex vivo ablations on bovine liver (the most proximal electrodes were used for ablations). (D) 3 Fr bipolar RF catheter used for ex vivo and in vivo ablations on porcine pancreas.

2.3. Protocol for ex vivo experiments

Three sets of ex vivo ablations were conducted, two on bovine liver and one on pancreatic tissue. Bovine liver was selected for its accessibility, homogeneity, and the ease of identifying the shape of the thermal lesions.

The first set of ex vivo ablations on liver was performed without pullback in order to tentatively establishing the relationship between the applied power, duration and created thermal lesion. This also allowed us to determine the approximate potential starting point for pullback, i.e., when the catheter pullback should start to avoid overheating and roll-off (abrupt rise in impedance). The applied voltage was 50 V and the ablation durations varied according to the roll-off time.

The second set of liver ablations was conducted with catheter pullback and provided information on the relation between pullback speed and lesion continuity. Both the first and second sets were conducted with the catheter between two fragments of liver (sandwich structure). The pullback sequence was guided by the impedance progress as follows: catheter pullback only started when impedance reached a plateau (ensuring sufficient heating of the tissue in contact with the electrodes) and with early signs of an imminent cut-out, i.e. when the impedance attempted to rise (implying overheating). In other words, the goal was to keep the impedance as steady as possible, since it is reasonable to assume that this implies that the same amount of power is being applied along the entire duct, hence ensuring the continuity of the thermal lesion without the need for overlapping. Pullback was carried out manually by the operator, who moved the catheter according to impedance progress as reflected in an audible signal provided by the RF generator. In this second set of ex vivo ablations the applied voltage was slightly lower (43 V instead of 50 V), since preliminary trials had shown that better pullback control could be obtained at this value. The liver ablations were conducted with a 5 Fr catheter as used in cardiac electrophysiology (see Figure 1(C)). Their durations varied with the length of the liver fragment.

Once the impedance-guided procedure was seen to be feasible, a third set of ablations was conducted on porcine pancreas. Sample size in this set was small ($n = 3$) due to a limited supply of ex vivo pancreatic specimens. Since it was not possible to introduce a 5 Fr catheter into the porcine duct, this set was finally conducted by a 3 Fr catheter (Minitrode, Bioampere Research, Conselve, Italy) with two 3 and 4 mm long 10 mm interspaced electrodes (Figure 1(D)). In this case the applied voltage was also 43 V, which implied a power of ~5 W.

2.4. Protocol for in vivo experiments

The ablation protocol established in the ex vivo trials was then tested on 8 Landrace-Large White pigs. This sample size was used in a previous study with a similar objective [7]. Prior to surgery, all the animals underwent a 12 h-fast. All were premedicated with azaperone (4 mg/kg intramuscularly (IM)) (Stresnil®, Ecuphar veterinaria, Spain), ketamine (10 mg/kg IM) (Ketamidor®, Richter Pharma, Austria) and morphine (0.2 mg/kg IM) (Morfina B.Braun®, B.Braun Medical, Spain).

Induction was performed with propofol 2–4 mg kg^{-1} intravenously (IV) (Propofol lipuro®, B.Braun Vetcare, Spain). After induction, all the animals were intubated with an orotracheal tube, and anesthesia was continued during the surgical procedure with isoflurane 2% (Isovet®, Piramal Critical Care Limited, UK) in 100% oxygen through a rebreathing circuit. Lactated Ringer's solution was infused at a rate of 10 ml/kg/h during the peri-operative period. Antibiotic therapy was administered with cephazoline 20 mg/kg IV (cefazolina normon®, Laboratorios Normon, Spain) via the cephalic vein. Heart rate, respiratory rate, pulse oximetry, electrocardiography, noninvasive blood pressure and capnography were monitored during anesthesia using a multi-parameter monitor (VetCare®, B Braun Vetcare, Spain).

Thermal ablations were performed with the same 3 Fr catheter as used on the ex vivo pancreas introduced into the duct through the pancreatic papilla by means of laparotomy and enterotomy. Once the catheter was placed in the end duct (~10 cm insertion depth), RF power (37 V) was applied. As in the ex vivo experiments, the catheter was pulled back along the entire duct until one of the electrodes was no longer inside it (RF generator automatically shut down). To control the pullback speed, the operator continuously monitored impedance visually on a laptop and by following the audible signal emitted by the RF generator.

After this process, enterotomy and laparotomy were closed in the conventional manner. The animals were kept alive for a 30-day follow-up, after which all were again anesthetized, intubated and ventilated for laparotomy and dissection of the entire pancreas, which was then immediately placed in 10% buffered neutral formalin. The animals were then euthanized using a commercial euthanasia solution. The principal duct of the dissected pancreas was identified and cannulated and the following tests were conducted: a feasibility test, consisting of reintroducing the catheter into the pancreatic duct through the duodenal papilla, and a permeability loss test consisting of injecting saline into the ablated duct. The pancreas was divided into 3 mm–thick sections for further histological analysis and 2 or 3 5 μm samples from each section were stained with hematoxylin and eosin and then evaluated by light microscopy. Pathologists unaware of the experimental design assigned the degree of exocrine pancreas atrophy from 0 to 5.

All the surgical procedures were performed by the same surgical team (AA and XM). To analyze sealing effectiveness, alterations of the animals' weight increments at 30 days after surgery, feasibility of reintroducing the catheter into the pancreatic duct, and duct permeability were considered. The degree of atrophy was determined by histological analysis.

3. Results

3.1. Ex vivo *experiments*

In the first set of ex vivo ablations on bovine liver (without pullback) initial impedance was 606 ± 14 Ω, and the mean applied power was ~5 W (50 V applied voltage). In all the ablations we observed a similar impedance pattern, which went through the following consecutive phases: 1) gradual initial impedance drop toward a steady minimum value, 2) plateau phase with a fairly steady minimum value, and 3) abrupt impedance rise. The beginning of the plateau phase occurred at 12 ± 3 s and coincided with the start of visible and audible signs of tissue overheating, such as steam pops, and also with a visible thermal lesion (tissue whitening). Impedance during the plateau was 384 ± 20 Ω. The abrupt impedance rise occurred at 21 ± 6 s and was preceded by audible pops 5 s before ablation ended.

The second set of ex vivo ablations employed the pullback technique and an attempt to keep a constant impedance value as long as possible, which meant keeping the plateau for as long as possible. The applied voltage was reduced to 43 V, since 50 V led to rapid tissue overheating, electrode sticking and a non-uniform lesion. As in the first set, the initial impedance and plateau impedance were 568 ± 48 Ω and 334 ± 37 Ω, respectively. In this case, due to the voltage reduction, applied power was ~5 W. In this second set we identified two main factors associated with pullback that affected lesion geometry and size: speed (slow vs. fast) and continuity (intermittent vs. uninterrupted –continuous–). A fast and continuous pullback caused an initial minor impedance drop and led to greater number of abrupt impedance rises, although without visible lesions. When pullback was slow, two different types of behavior were seen that depended on pullback continuity:

1. When pullback was slow and intermittent, impedance followed a sawtooth waveform with small abrupt rises (see black arrow in Figure 2(A)) each time the catheter was moved, so that the evolution matched well with the lesion pattern. The intermittency involved tissue charring and sticking just before the end of pullback, or at extremely low speed, while gaps appeared (absence of thermal lesion) with a fast pullback.
2. When pullback was slow and continuous, the impedance waveform smoothed out (see Figure 2(B)) and avoided tissue sticking. The lesions thus produced were also uniform in depth, with a whitish zone extending continuously ~1 mm around the electrode along the entire ablation line (see Figure 2(D)). In these cases the plateau was reached in ~23 s, after which pullback was applied at a mean speed of ~0.07 cm/s. When the speed became too slow, impedance gradually rose (black arrow in Figure 2(C)), which was interpreted as an early sign of an imminent impedance jump (implying overheating) and therefore pullback was speeded up.

The third set of ex vivo ablations was conducted on pancreatic tissue with a 3 Fr instead of a 5 Fr catheter, since the pancreatic lumen was narrower than expected. The initial impedance was 523 ± 29 Ω, a value slightly lower than that obtained by a 5 Fr catheter on bovine liver. The applied voltage was kept at the same level as in the previous set (~43 V). Impedance followed the three-phase pattern observed in the first two sets of ex vivo ablations. The time to reach plateau was more than 100 s, which was three times longer than in the two previous sets. The impedance value

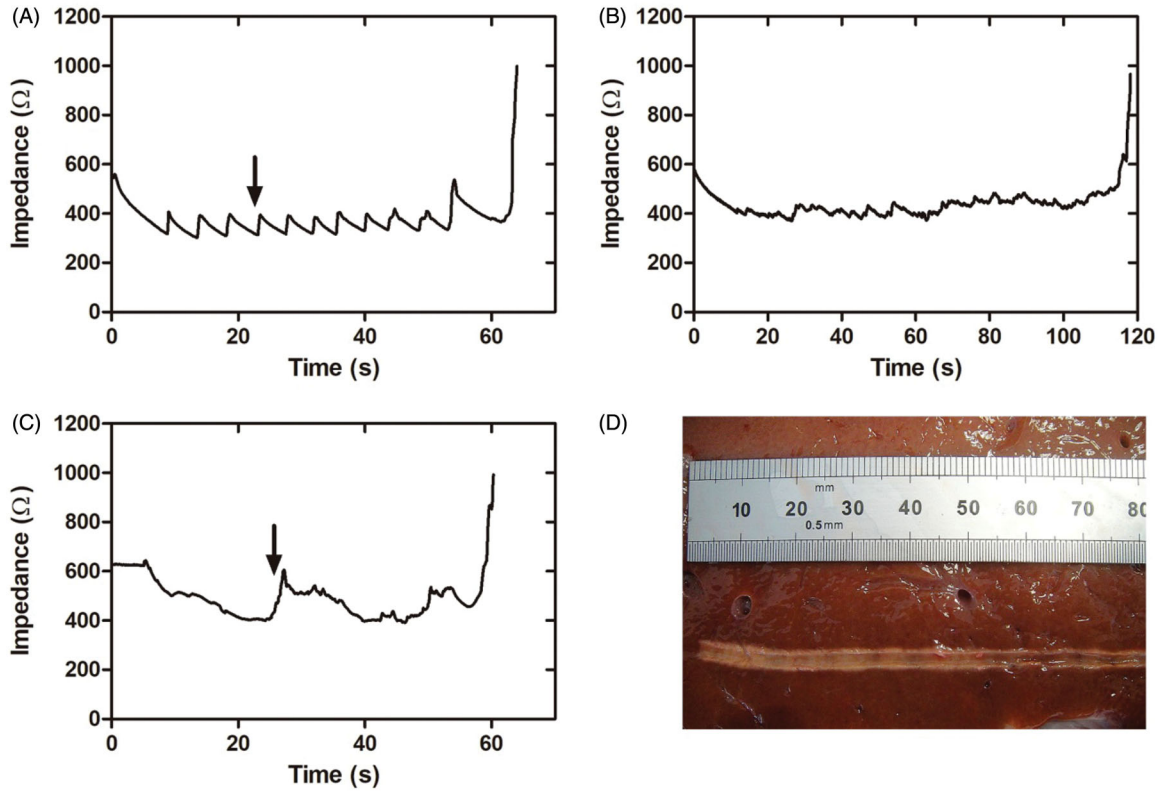

Figure 2. Results of the second set of ex vivo experiments. (A–C) Examples of impedance evolution (A). Small-amplitude sawtooth associated with slow and intermittent catheter pullback; (B and C). Smooth patterns associated with slow and continuous catheter pullback. (D) Thermal lesion created on bovine liver by slow and continuous pullback (impedance shown in B).

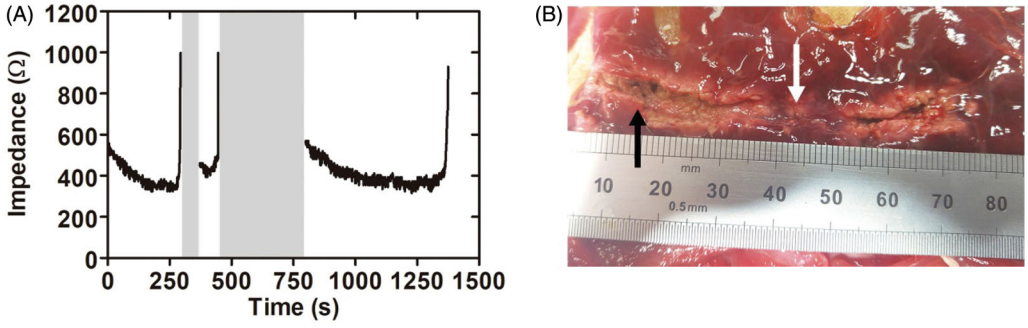

Figure 3. Results of the third set of ex vivo experiments. (A) Typical impedance during ablation. (B) Lesion created along the pancreatic duct in a pancreas treated with 43 V and pullback as continuous as possible. Gray bands show power cut off instants after abrupt impedance increases associated with tissue sticking and carbonization (black arrow in B). After this event pullback was always speeded up in order to relocate the catheter, which in turn led to some visible gaps (white arrow in B).

at the plateau was 302 ± 40 Ω (see Figure 3(A)). Abrupt impedance increases were associated with tissue sticking and carbonization points (see black arrow in Figure 3(B)), just after which the catheter was relocated. Unfortunately, this movement caused visible gaps (see white arrow in Figure 3(B)), since they were associated exactly with the zones where the electrodes did not apply power as the catheter was moved. As in the previous sets, we also observed that pulling back too fast impeded the creation of visible thermal lesions. Overall, the lesions created in this third set showed larger margins (2–3 mm) than the two previous sets on liver with a 5 Fr catheter. During the ablations, more abrupt impedance changes and more roll-offs occurred, which contributed to a more intermittent pullback and to irregular lesions in terms of depth and continuity (i.e. with gaps).

3.2. In vivo *experiments*

Since the tissue lesions of the *in vivo* group could not be seen until 30 days after the procedure, the evolution of the electrical variables was the only indicator for creating uniform and continuous thermal lesions. The mean initial impedance was 308 ± 60 Ω, considerably lower than in the ex vivo specimens. The applied voltage was reduced to 37 V, which implied a power of ∼5 W (comparable to the value measured in ex vivo ablations). A time of ∼30 s was required

to reach the impedance plateau ($220 \pm 35\,\Omega$), at which time pullback started. Impedance followed the same three-phase pattern as in the ex vivo ablations. However, the *in vivo* ablations showed a higher incidence of roll-offs, estimated as one every 40 s of ablation, and the impedance rises usually involved tissue sticking, which forced us to relocate the catheter rapidly in order to complete the ablation, which often required vigorous action. This meant the impedance evolution was more irregular than in the ex vivo experiments. Total ablation duration varied slightly in the trials in relation to specific duct length and roll-off occurrence. An average of 11 cm of pancreatic duct was ablated at a mean pullback speed of ~0.1 cm/s.

During the 30-day follow-up the animals experienced alterations of stool consistency. After this period, their mean weight was 31 kg, which meant a slower than normal rate of weight gain (4 kg per 30 days). At necropsy, the feasibility test to verify the presence of ductal occlusion failed, since it was impossible to re-insert more than a few centimeters of the catheter into the duct, due to the lumen being too narrow. This also meant we could not perform the permeability test, as the liquid could not be injected as planned through the distal end of the duct. All this suggested that sealing was completely effective after 30 days at the level of the duodenal papilla. Beyond the papilla, a macroscopic view of cross-sections of pancreatic duct revealed different degrees of ductal dilation (diameter ranging widely from <1 mm to >10 mm), although at the level of the head the lumen seemed completely sealed in all cases (Section A in Figure 4).

Figure 5 shows histological images of normal pancreatic tissue and pancreas after treatment. The histological study of the treated samples revealed complete acinar atrophy and that only the intralobular ducts remained after ductal ablation (Figure 5(D,E)). The epithelium of the interlobular and some of the intralobular ducts showed a metaplasia from columnar or cuboidal to squamous and was lost in other areas (Figure 5(F)). All the samples showed marked periductal and interlobular fibrosis (Figure 5(D–F)) and scattered inflammatory infiltrate (Figure 5(F)).

4. Discussion

Sealing the pancreatic duct has always been challenging due to the risk of pancreatic juice leaking into the peritoneal cavity, which continues to be the main complication contributing to the high mortality rate [7]. The endoluminal RFA with pullback proposed here could potentially reduce this risk. Moreover, being a minimally-invasive technique, it offers the advantages of a likely faster recovery and fewer side effects than injecting a sealing agent or tissue suturing. To our knowledge, this is the first study to examine the feasibility of the catheter-based RF sealing technique for the pancreatic duct. As this was a development study, it had several phases to progressively fine-tune the proposed technique (catheter and ablation protocol) and finally obtain relevant information on its safety and performance on an *in vivo* porcine model.

4.1. Initial steps fine-tuning technique

The first phases conducted on liver ex vivo fragments showed how the different variables involved interact with each other during ablation with pullback. What we learned

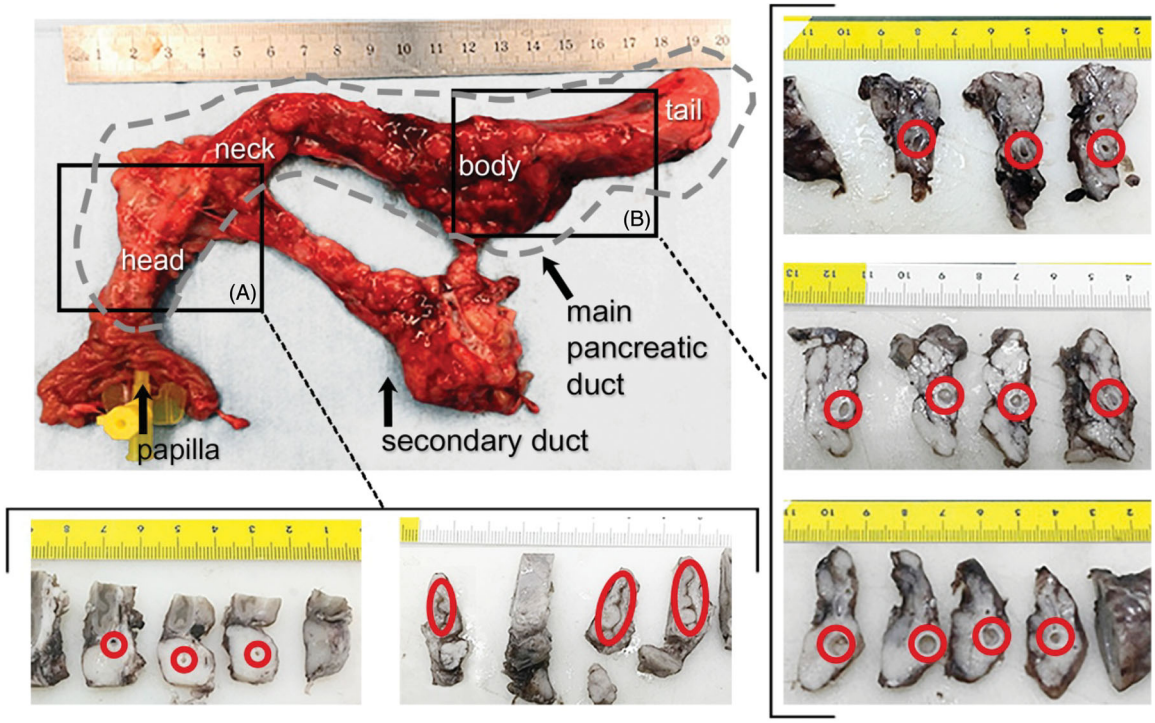

Figure 4. Results of the in vivo experiments. Macroscopic images of one of the treated pancreas and cross sections at the level of the head (A) and body (B). Red circles indicate the position of the main duct. Lumen was not completely closed in all cases and ductal dilation was observed, particularly in the body (units in cm). Gray dashed line indicates the main duct position in pancreas.

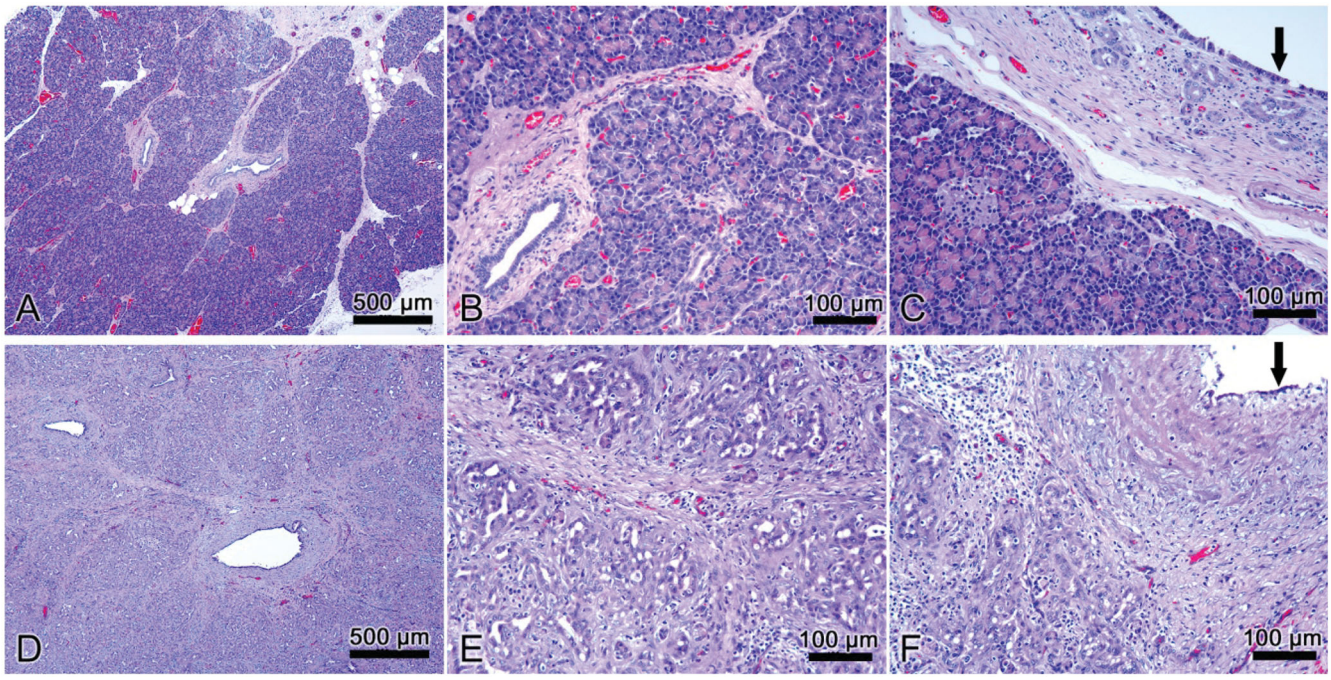

Figure 5. Results of in vivo experiment. Histological images of normal pancreas (A, B, C) and samples with sealing-induced pancreatic atrophy (D, E, F). Compared to normal pancreatic tissue, the treated samples show evident atrophy of the acinar component (purple dye) with only intralobular ducts remaining (D, E); the epithelium of the interlobular ducts is flattened or has been lost (F, black arrow); marked interlobular fibrosis (D, E; F); scattered inflammatory infiltrate (E, F). H&E × 5 (A, D) and ×20 (B, C, E, F).

was that: (1) a few watts (∼5 W) are enough to create 1–2 mm deep lesions; (2) pullback must begin when the impedance plateau is reached, which may coincide with audible pops; (3) it is possible to modulate the rate of pullback to keep the impedance as steady as possible, i.e. to try to maintain the plateau phase during the entire procedure; (4) this can be done by monitoring impedance and/or by an audible signal associated with impedance progress; and (5) if all these conditions are observed, the thermal lesion can be continuous (without gaps) along the entire path.

When we tried to transfer these conditions to the case of the pancreatic duct (pancreas ex vivo ablations), we learned that: (1) a narrower catheter diameter is required (3 Fr instead of 5 Fr); (2) catheter pullback through the pancreatic duct is less straightforward than the simple movement between two slices of liver tissue; (3) this means that the impedance-guided lesion is not so effective in the pancreas, with sticking, a need for overlap, and possible gaps; (4) sudden impedance rises are possibly related to tissue sticking and require moving the catheter, with the possibility of gaps; (5) gaps can be also produced by excessive pullback speed; and (6) when present, thermal lesions are 2–3 mm deep. This information was used to carry out a 30-day survival *in vivo* study.

4.2. Clinical assessment of the technique

On planning the *in vivo* study we expected thermal ablation inside the pancreatic main duct to produce the following phenomena: (1) occlusion of the small exocrine ducts branching from the main duct and subsequent acinar atrophy, causing the suppression of exocrine secretions; and (2) shrinkage of the collagen fibers around the main duct and subsequent reduction of its lumen, making it less permeable. Initially we thought that in order for these phenomena to occur efficiently, a continuous thermal lesion had to be created along a segment of the main duct. This was probably over-optimistic, since although thermal ablation produces immediate tissue shrinkage (due to protein denaturation and collagen contraction) this could only create a partial occlusion, as opposed to other mechanical methods (such as suture or stapler).

What the *in vivo* study revealed is that it is very difficult to create continuous lesions along the pancreatic duct, possibly due to the irregular anatomy of the main duct, but also due to the technical limitations of the impedance-guided protocol. In fact, gaps were observed in the ex vivo pancreas just after ablation. In the same way, the sudden impedance rises during *in vivo* ablations suggest the possible presence of gaps in the lesion and the possibility of the diameter not being reduced along the whole ablation length. This was later confirmed in the macroscopic analysis, where the main duct was not completely occluded in all zones. Complete duct occlusion at the pancreas head was also evident from the impossibility of reinserting the catheter through the duodenal papilla. We still do not have a convincing explanation of why the proximal duct (head zone) was more occluded than the distal duct. The images in Figure 4 also show that the ablated duct was usually circular in shape, regardless of the dilation diameter or location, which suggests that the energy deposition occurred symmetrically around the electrodes and was limited in depth.

Interestingly, despite the existence of lesion gaps and presence of non-occluded segments, clinical observations during follow-up and histological findings were compatible

with complete exocrine atrophy. The atrophic pancreas was deprived of acini to secrete digestive enzymes, which caused the failure of the digestive functions. All the animals experienced digestive alterations and a notably reduced rate of weight gain after the 30-day follow-up.

In view of all the results, the complete occlusion of the entire main duct may not be required to generate complete exocrine atrophy. In fact, it is possible that the partially occluded duct segments also contributed to the exocrine atrophy. Since RF ablation also severs duct walls and produces thermal necrosis and apoptosis of the ablated zone, it is likely that atrophy and acinar cell loss are also a result of thermally-induced apoptosis. It is thus reasonable to assume that a fully continuous lesion along the main duct might not be necessary to achieve exocrine atrophy, which would be triggered not only by an immediate RF-induced effect, but also by biological processes within 30 days after ablation.

4.3. Safety issues

Regarding the safety issues involved in the ablative technique, we must keep in mind that bipolar RFA has already been clinically used for endoluminal ablation of vessels and biliary duct, so the concept of endoluminal ablation itself is well-known and assumed to be safe. The risks of using RFA instead of another mechanical method, such as staplers, sutures or clips, could include overheating of the target tissue and unintentional ablation of the neighboring tissue (e.g. intestine). In our study these risks were minimized by establishing a 'safe ablation environment' by trying to keep the pancreas as far as possible from other viscera during ablation by simple mechanical deviation. In addition, all the procedures were accomplished by personnel experienced in using RF-based devices. Finally, the absence of postoperative complications associated with RF power suggests that the proposed ablation method keeps risks at a reasonably low level.

4.4. Technical feasibility

The ablation control proposed in this study is entirely based on impedance progress. We discarded temperature monitoring due to it being technically complex to include temperature sensors in such a small catheter. Moreover, while a temperature sensor would only provide information on the temperature in the tissue in contact with it (not necessarily the maximum tissue temperature), impedance gives a more complete picture of the characteristics of tissue affected by ablation through the direct relationship between electrical conductivity and temperature. In fact, this technique has been used previously in the management of biliary tumors and venous obstruction or other venous insufficiencies [10–13]. While we designed our own endoluminal RFA protocol, other studies used commercial devices designed for treating varicose veins (e.g. Celon ProCurve, Olympus, Germany). In both cases the method is based on impedance feedback for catheter guidance by visualizing impedance and power evolution and attending to audible signals. It also allows working in a specific impedance range that cuts out when exceeded. We had to adapt this technique to the present study, since endoluminal RFA had never been used before to seal the pancreatic duct. The delicate pancreatic tissue structure required a flexible applicator and the right catheter to fit a ~1 mm duct diameter, which ruled out the use of the commercial product of 5 Fr.

In addition, impedance monitoring has already been proposed to estimate the temperature and lesion size during RF ablation due to the inverse relationship of both parameters [14]. Tissue heating enhances ion mobility and current flow and thus produces a characteristic impedance drop in the early stages of ablation. Although thermal lesions in high-temperature ablative techniques require temperatures in the range 50–100 °C, it is also known that lesion evolution is closely connected to the temperature-time relationship, which depends on the amount of power applied. In particular, it is known that a few minutes of exposure at 50 °C triggers progressive tissue shrinkage and irreversible tissue damage [15], while only a few seconds at 60 °C produce tissue coagulative necrosis seen as a whitish area in the ablation zone [16,17]. Once thermal equilibrium has been reached, the impedance value stabilizes at the minimum and lesion size remains static. Further ablation leads to tissue overheating and vaporization at temperatures between 100 and 105 °C and is characterized by audible steam pops, an abrupt impedance rise, tissue carbonization and sticking [17]. Once focused on impedance monitoring, our findings identified three different phases in its progress during ablation: 1) a drop associated with initial heating, 2) a plateau phase, and 3) occasional abrupt increases associated with overheating. All the phases could easily be distinguished in our ex vivo findings, in which whitish and carbonization zones appeared, suggesting that the tissue was in fact exposed to the 60–100 °C range. Overheating incidents also occurred in the *in vivo* study and suggest that the tissue was exposed to temperatures of up to 100 °C. The longer the plateau phase, the longer the ablation with sufficient power delivery and without carbonization. It has also been suggested that keeping the plateau impedance at a target value for a specific time should lead to the desired lesion depth [9]. The value of the plateau phase depends on tissue type and other conditions that affect its electrical properties, such as hydration or blood irrigation [18,19]. For instance, in our study the differences between the ex vivo and *in vivo* models were possibly related to additional heat loss by convective blood perfusion cooling (also known as heat sink effect), which is only present under *in vivo* conditions. Other factors could also have affected these differences, such as a smaller impedance drop and a higher threshold temperature for coagulative necrosis, finally producing smaller lesion depths in the *in vivo* case. Accordingly, we observed that *in vivo* samples had nearly half as low initial impedance values ($308 \pm 60\,\Omega$ vs $523 \pm 29\,\Omega$) and a smaller impedance drop ($220 \pm 35\,\Omega$ vs $302 \pm 40\,\Omega$ at plateau) than ex vivo specimens. We were not able to assess the differences in lesion depth between ex vivo and *in vivo* cases since in the latter case the lesion dimensions were assessed after a 30-day follow-up

period. However, our findings can be discussed in the light of previous liver studies (with a similar pancreas blood perfusion rate, 860 ± 170 ml/min/kg vs. 767 ± 357 ml/min/kg [20]). These studies showed that *in vivo* lesions have a 36–44% smaller diameter than ex vivo lesions [21–23], which suggests that the *in vivo* pancreatic lesions created in our study could be around 1 mm deep (since lesion depth was 2–3 mm in the ex vivo case and similar power levels were used in both cases).

Additionally, different studies have reported that tissue shrinkage (which starts at 50 °C) produces up to 20–30% of tissue constriction of the initial margin and therefore the real ablation zone is actually greater than that measured [15,24,25], while a limited degree of tissue shrinkage could also reduce the chances of complete mechanical occlusion of the duct, although, as seen in our study, it was sufficient to reduce the duct diameter to less than the catheter diameter and ruled out catheter reintroduction.

Due to variations in the electrical properties of ex and *in vivo* tissue, a lower voltage value was used in the *in vivo* study (43 V vs. 38 V). This change also affected the pullback speed (∼0.03 cm/s vs. 0.1 cm/s), but in all cases a power of ∼5 W could be delivered, suggesting that the delivered power, as determined by applied voltage and pullback speed, is the vital parameter in achieving successful RFA. The power and pullback speed values used in our study were noticeably lower than those usually reported for venous ablation (18–25 W and 0.5–1 cm/s, respectively) [9,12,13,26,27]. Numerous studies have reported that the recommended clinical power and pullback speed values can increase the incidence of tissue carbonization and sticking [12]. An additional issue in obtaining permanent sealing is the need to reapply the treatment (overlapping) to provide sufficient energy for effective sealing [28]. Interestingly, Badham et al. [12] suggested that values of 6 W and 0.08 cm/s are the most optimal to obtain a successful vein lesion by single RF ablation and avoid tissue overheating and sticking. These values are very similar to these employed by us (5 W, 0.03–0.1 cm/s). It is important to note that while we aimed for a slow continuous pullback, Badham et al. used a discontinuous pullback, so that 0.08 cm/s was really an approximate value. This similarity could be owing to the electrical properties of both tissues. In the *in vivo* study we found that a large number of abrupt impedance increases and tissue sticking events were inevitable. This problem could pose a serious risk of soft tissue rupture during the treatment. The relationship between the applied power and pullback speed determines the required energy level and the rate at which it is delivered to the tissue, and thus the final thermal dose to cause tissue damage. The optimization of these parameters is still pending.

The outcomes obtained from this technique are undoubtedly affected by the additional factor of the operator's skill in controlling catheter pullback [26]. As already mentioned, an excessively slow pullback implies greater power deposited in the target area together with carbonization and sticking, while an exceedingly fast pullback produces gaps or even no lesion at all. Although the manufacturers usually recommend the appropriate powers and speeds to obtain continuous lesions and avoid overheating, the inherent tissue heterogeneity impedes creating a uniform lesion along the entire path. The operator's skill thus plays a vital role in varying pullback speed according to the impedance variations encountered. The amount of delivered power and pullback speed will also vary according to the desired outcome and may differ from the manufacturer's recommendations [27,28]. For all these reasons it is important to first estimate the relationship between impedance, delivered power and the required thermal lesion before applying endoluminal RFA with pullback.

4.5. Limitations of the study

Although our final clinical objective is the management of the pancreatic stump, the *in vivo* study was conducted on a non-transected pancreatic duct. A transected pancreas model would be more complex and would entail a higher risk of pancreatic leakage. Further research on this matter should therefore be conducted involving endoluminal RF sealing of the transected pancreatic duct in order to confirm the feasibility of the technique on a more realistic model.

As regards the clinical implications, it is important to note that the porcine model used in this study is anatomically different to the human pancreas in certain respects, as it has a secondary duct branching out from the main pancreatic duct (see Figure 1 from [7]). In our study this duct was not ablated and therefore maintained its enzymatic secretory function, which could have reduced the effectiveness of the proposed technique. For this very reason, the technique could be even more effective in the human pancreas.

5. Conclusions

The impedance-guided endoluminal RFA technique designed to seal the pancreatic duct seems to be a promising, feasible and safe alternative for management of the pancreatic stump and reducing the risk of leakage. Although power and pullback speed still need to be optimized, the findings obtained suggest that a fully continuous RFA lesion along the entire duct may not in fact be required to achieve pancreatic atrophy.

Disclosure statement

All authors have no conflict of interest or financial ties to disclose.

Funding

This work was supported by the Spanish Ministerio de Economía, Industria y Competitividad under "*Plan Estatal de Investigación, Desarrollo e Innovación Orientada a los Retos de la Sociedad*" (Grant TEC2014–52383–C3–R) and by the Spanish Ministerio de Ciencia, Innovación y Universidades under "*Programa Estatal de I+D+i Orientada a los Retos de la Sociedad*" (Grant: RTI2018-094357-B-C21 and –C22). Elżbieta Ewertowska has a Predoctoral Grant (BES-2015–073285) from the Ministry of Economy, Industry and Competitiveness (Government of Spain). Also funding was received from Secretaría de Estado de Investigación, Desarrollo e Innovación.

ORCID

Dolors Fondevila http://orcid.org/0000-0001-6651-3173
Rita Quesada http://orcid.org/0000-0002-8264-0356
Macarena Trujillo http://orcid.org/0000-0003-4145-2188
Fernando Burdío http://orcid.org/0000-0003-3038-0086
Enrique Berjano http://orcid.org/0000-0002-3247-2665

References

[1] Schneider MU, Meister R, Domschke S, et al. Whipple's procedure plus intraoperative pancreatic duct occlusion for severe chronic pancreatitis: clinical, exocrine, and endocrine consequences during a 3-year follow-up. Pancreas. 1987;2:715–726.
[2] Alfieri S, Quero G, Rosa F, et al. Indications and results of pancreatic stump duct occlusion after duodenopancreatectomy. Updates Surg. 2016;68:287–293.
[3] Tran K, Van Eijck C, Di Carlo V, et al. Occlusion of the pancreatic duct versus pancreaticojejunostomy: a prospective randomized trial. Ann Surg. 2002;236:422–428.
[4] Schoellhammer HF, Fong Y, Gagandeep S. Techniques for prevention of pancreatic leak after pancreatectomy. Hepatobiliary Surg Nutr. 2014;3:276–287.
[5] Quesada R, Burdío F, Iglesias M, et al. Radiofrequency pancreatic ablation and section of the main pancreatic duct does not lead to necrotizing pancreatitis. Pancreas. 2014;43:931–937.
[6] Quesada R, Andaluz A, Cáceres M, et al. Long-term evolution of acinar-to-ductal metaplasia and b-cell mass after radiofrequency-assisted transection of the pancreas in a controlled large animal model. Pancreatology. 2016;16:38–43.
[7] Burdío F, Dorcaratto D, Hernandez L, et al. Radiofrequency-induced heating versus mechanical stapler for pancreatic stump closure: *in vivo* comparative study. Int J Hyperthermia. 2016;32:272–280.
[8] Khorsandi SE, Kysela P, Valek V, et al. Initial data on a novel endovascular radiofrequency catheter when used for arterial occlusion in liver cancer. Eur Surg. 2009;41:104–108.
[9] Reich-Schupke S, Mumme A, Stücker M. Histopathological findings in varicose veins following bipolar radiofrequency-induced thermotherapy-results of an ex vivo experiment. Phlebology. 2011;26:69–74.
[10] Atar M, Kadayifci A, Daglilar E, et al. Ex vivo human bile duct radiofrequency ablation with a bipolar catheter. Surg Endosc. 2018;32:2808–2813.
[11] Duben J, Hnatek L, Dudesek B, et al. Bipolar radiofrequency-induced thermotherapy of haemorrhoids: a new minimally invasive method for haemorrhoidal disease treatment. Early results of a pilot study. Wideochir Inne Tech Maloinwazyjne. 2013;8:43–48.
[12] Badham GE, Dos Santos SJ, Whiteley MS. Radiofrequency-induced thermotherapy (RFiTT) in a porcine liver model and ex vivo great saphenous vein. Minim Invasive Ther Allied Technol. 2017;26:200–206.
[13] Tesmann JP, Thierbach H, Dietrich A, et al. Radiofrequency induced thermotherapy (RFITT) of varicose veins compared to endovenous laser treatment (EVLT): a non-randomized prospective study concentrating on occlusion rates, side-effects and clinical outcome. Eur J Dermatol. 2011;21:945–951.
[14] Hartung WM, Burton ME, Deam AG, et al. Estimation of temperature during radiofrequency catheter ablation using impedance measurements. Pacing Clin Electrophysiol. 1995;18:2017–2021.
[15] Rossmann C, Garrett-Mayer E, Rattay F, et al. Dynamics of tissue shrinkage during ablative temperature exposures. Physiol Meas. 2014;35:55–67.
[16] Goldberg SN, Gazelle GS, Mueller PR. Thermal ablation therapy for focal malignancy: a unified approach to underlying principles, techniques, and diagnostic imaging guidance. AJR Am J Roentgenol. 2000;174:323–331.
[17] Thomsen S. Pathologic analysis of photothermal and photomechanical effects of laser-tissue interactions. Photochem Photobiol. 1991;53:825–835.
[18] Haemmerich D, Ozkan OR, Tsai JZ, et al. Changes in electrical resistivity of swine liver after occlusion and postmortem. Med Biol Eng Comput. 2002;40:29–33.
[19] Shahzad A, Khan S, Jones M, et al. Investigation of the effect of dehydration on tissue dielectric properties in ex vivo measurements. Biomed Phys Eng Express. 2017;3:045001.
[20] Hasgall PA, Di Gennaro F, Baumgartner C, et al. 2016. IT'IS Database for thermal and electromagnetic parameters of biological tissues, Version 3.0, September 1st, 2015. [cited 2019 May 19] Available from: www.itis.ethz.ch/database.
[21] Patterson EJ, Scudamore CH, Owen DA, et al. Radiofrequency ablation of porcine liver *in vivo*: effects of blood flow and treatment time on lesion size. Ann Surg. 1998;227:559–565.
[22] Song KD, Lee MW, Park HJ, et al. Hepatic radiofrequency ablation: *in vivo* and ex vivo comparisons of 15-gauge (G) and 17-G internally cooled electrodes. Br J Radiol. 2015;88:20140497.
[23] Goldberg SN, Hahn PF, Halpern EF, et al. Radio-frequency tissue ablation: effect of pharmacologic modulation of blood flow on coagulation diameter. Radiology. 1998;209:761–767.
[24] Brace CL, Diaz TA, Hinshaw JL, et al. Tissue contraction caused by radiofrequency and microwave ablation: a laboratory study in liver and lung: tissue contraction caused by thermal ablation. J Vasc Interv Radiol. 2010;21:1280–1286.
[25] Yu MH, Kim YJ, Park HS, et al. Shrinkage of hepatocellular carcinoma after radiofrequency ablation following transcatheter arterial chemoembolization: analysis of contributing factors. PLoS One. 2019;14:e0210667.
[26] Braithwaite B, Hnatek L, Zierau U, et al. Radiofrequency-induced thermal therapy: results of a European multicentre study of resistive ablation of incompetent truncal varicose veins. Phlebology. 2013;28:38–46.
[27] Badham GE, Dos Santos SJ, Lloyd LBA, et al. One-year results of the use of endovenous radiofrequency ablation utilising an optimized radiofrequency-induced thermotherapy protocol for the treatment of truncal superficial venous reflux. Phlebology. 2018;33:298–302.
[28] Newman JE, Meecham L, Walker RJ, et al. Optimising treatment parameters for radiofrequency induced thermal therapy (RFiTT): a comparison of the manufacturer's treatment guidance with a locally developed treatment protocol. Eur J Vasc Endovasc Surg. 2014;47:664–669.